ELSEVIER

International Journal of Solids and Structures 41 (2004) 1801–1822

INTERNATIONAL JOURNAL OF SOLIDS and STRUCTURES

www.elsevier.com/locate/ijsolstr

Dynamic effects of moving load on a poroelastic soil medium by an approximate method

D.D. Theodorakopoulos, A.P. Chassiakos, D.E. Beskos *

Structural Engineering Division, Department of Civil Engineering, University of Patras, GR-26 500 Patras, Greece

Received 12 June 2003; received in revised form 23 September 2003

Abstract

The problem of the dynamic response of a fully saturated poroelastic soil stratum on bedrock subjected to a moving load is studied by using the theory of Mei and Foda under conditions of plane strain. The applied load is considered to be the sum of a large number of harmonics with varying frequency in the form of a Fourier expansion. The method of solution considers the total field to be approximated by the superposition of an elastodynamic problem with modified elastic constants and mass density for the whole domain and a diffusion problem for the pore fluid pressure confined to a boundary layer near the free surface of the medium. Both problems are solved analytically in the frequency domain. The effects of the shear modulus, permeability and porosity of the soil medium and the velocity of the moving load on the dynamic response of the soil layer are numerically evaluated and compared with those obtained by the exact solution of the problem. It is concluded that for fine poroelastic materials, the accuracy of the present method against the exact one is excellent.

Keywords: Poroelastic soil; Outer approximation; Boundary layer correction; Porosity; Permeability; Shear modulus; Moving load; Fourier series; Vertical displacement; Pore pressure; Vertical effective stress

1. Introduction

The study of the dynamic behavior of a half-space soil medium under the action of moving loads on its free surface is of significant importance in the area of geotechnical/structural transportation facilities and has thus received a great attention over the past decades. Depending on the degree of modeling elaboration of the soil medium used in the analysis, one can distinguish three categories among the existing published methods for determining the dynamic response of the ground surface due to moving loads. In the first category the soil is modeled as a system of Winkler springs, while in the second category the soil is modeled as a linear elastic or viscoelastic, homogeneous or layered half-space. Finally, in the third category, the soil medium can be inelastic, poroelastic or gradient elastic. A comprehensive review of the relevant works in each category can be found in Theodorakopoulos (2003).

* Corresponding author. Tel.: +30-61-997-654; fax: +30-61-997-812.
E-mail address: d.e.beskos@upatras.gr (D.E. Beskos).

0020-7683/$ - see front matter © 2003 Elsevier Ltd. All rights reserved.
doi:10.1016/j.ijsolstr.2003.11.009

So far, the most comprehensive analytical/numerical works on the dynamic response of a poroelastic half-space to moving loads under conditions of plain strain are those presented by Siddharthan et al. (1993), based on the assumption of no relative motion between solid and fluid constituents and by Theodorakopoulos (2003), accounting for the full generality of Biot's (1956) governing field equations. In the latter contribution, the exact vertical soil displacements and stresses as well as the pore water pressure of a poroelastic soil layer on rigid bedrock subjected to a strip load moving at constant velocity were explicitly expressed and numerically evaluated for various values of shear modulus, compressibility of fluid, porosity, permeability and load speed. Thus, a detailed assessment of the relative importance of those parameters on the response was accomplished.

However, the exact analytical solution of the above problem was rather complicated. In an effort to obtain an approximate analytical solution of the same problem, characterized by simplicity and satisfactory accuracy, the method of Mei and Foda (1981) was employed in this paper. Among the applications of Mei and Foda's (1981) theory in soil dynamics, one can mention the works of Mei and Foda (1981), Foda and Mei (1983), Mei et al. (1984) and more recently of Theodorakopoulos et al. (2001) in conjunction with analytical techniques and those of Kattis et al. (1998, 1999, 2003) in conjunction with boundary elements.

According to the arguments of Mei and Foda (1981) in regions not too close to a free surface, the fluid and solid matrix move as a whole due to the large frictional resistance forces in the pores of the medium. However, relative fluid-motion is appreciable within a thin boundary layer near the free surface because of the easiness with which the fluid can squeeze in or out of the free surface. Thus, a given poroelastic problem involving a free surface can be approximately solved by first solving an elastodynamic outer problem with modified elastic constants and mass density for the whole domain and then making a simple correction near the free surface.

Thus, in this work the problem of determining the dynamic response of a uniform, fully saturated poroelastic soil layer on rigid bedrock subjected to a moving strip load is solved under conditions of plane strain by the aforementioned approximate method of Mei and Foda (1981). The distributed load, which moves at constant velocity, is expanded in Fourier series as in Siddharthan et al. (1993) and Theodorakopoulos (2003). The outer approximation, i.e., the modified elastodynamic solution for the whole domain, as well as the boundary layer correction resulting in the solution of a diffusion problem for the pore fluid pressure, are both obtained analytically/numerically. The results are compared against those of the exact method in Theodorakopoulos (2003) in order to establish the range of the various parameters of the problem for which the accuracy of this approximate method is satisfactory.

2. System considered and moving load representation

The soil system examined and the applied moving load are shown in Fig. 1. The system consists of a uniform poroelastic soil layer, fully saturated by a viscous fluid, under conditions of plane strain. The fluid is free to squeeze in and out of the entire upper soil surface. The soil layer has a height H and is fully bonded on a rigid and impervious bedrock.

For the sake of comparison, the applied load condition and configuration are the same as in Siddharthan et al. (1993) and Theodorakopoulos (2003). More specifically, the surface vertical strip load moves at a constant velocity c, has a width $2\ell = 4.0$ m, a constant intensity $F(x) = F = 400.000$ N/m^2 and is considered to be periodic with wave length $2L = 409.6$ m (Fig. 1). This applied load is assumed to be expanded in a Fourier series of the form

$$\begin{aligned} F(x-ct) &= \mathrm{Re}\sum_{n=-\infty}^{\infty} F_n \mathrm{e}^{\mathrm{i}\lambda_n(x-ct)} \quad \text{for } t>0 \\ F(x) &= \mathrm{Re}\sum_{n=-\infty}^{\infty} F_n \mathrm{e}^{\mathrm{i}\lambda_n x} \quad \text{for } t=0 \end{aligned} \tag{1}$$

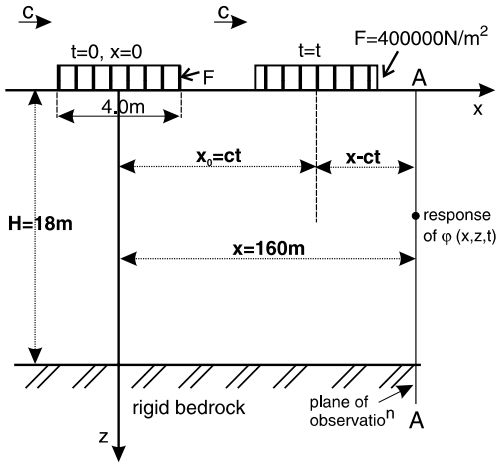

Fig. 1. Geometry of traveling surface load and plane of observation.

where Re denotes the real part and the harmonics F_n and the parameter λ_n vary with n. The entire loading function, including the "quiet zone" needed for the attenuation of the response due to a passing load before the beginning of the next cycle, is sampled at $2N + 1$ equally spaced points ($\Delta x = 0.1$), numbered from zero to $2N = 4096$. Thus, in accordance with Theodorakopoulos (2003), the discretized loading function of Eq. (1) may be expressed as a linear combination of $N + 1 = 2049$ harmonics of the form

$$F(x - ct) = \mathrm{Re} \sum_{n=0}^{2048} F_n \mathrm{e}^{\mathrm{i}\lambda_n (x-ct)} \tag{2}$$

where

$$F_n = \begin{cases} \frac{\ell}{L} F & \text{for } n = 0 \\ 2\frac{1}{n\pi} \sin\left(n\pi \frac{\ell}{L}\right) F & \text{for } n > 0 \end{cases} \tag{3}$$

and

$$\lambda_n = n\frac{\pi}{L} \tag{4}$$

Eq. (4) indicates that λ_n varies from zero for $n = 0$, to $10\pi = 31.41$ for $n = 2048$. It should be mentioned here that the limitation on the number of harmonics in the Fourier expansion of the applied load from infinity in Eq. (1) to 4096 in Eqs. (2) and (3) does not affect the accuracy of the response of the system, since the response contributions associated with high values of λ_n are small (Siddharthan et al., 1993; Theodorakopoulos, 2003).

3. Governing equations of motion of the soil system

Assuming plane strain conditions and referring to the rectangular system of co-ordinates x, z shown in Fig. 1, the linearized dynamic equations of motion of a fully saturated poroelastic medium due to Biot (1956) in the notation of Mei and Foda (1981), under the assumption of an incompressible solid constituent and neglecting the inertia mass coupling terms, are given as

$$\frac{\vartheta\tau_x}{\vartheta x}+\frac{\vartheta\tau_{xz}}{\vartheta z}+\frac{f^2}{k}(\dot{u}^{\mathrm{f}}-\dot{u})-(1-f)\frac{\vartheta p}{\vartheta x}=(1-f)\rho_{\mathrm{s}}\ddot{u} \tag{5}$$

$$\frac{\vartheta\tau_z}{\vartheta z}+\frac{\vartheta\tau_{xz}}{\vartheta x}+\frac{f^2}{k}(\dot{w}^{\mathrm{f}}-\dot{w})-(1-f)\frac{\vartheta p}{\vartheta z}=(1-f)\rho_{\mathrm{s}}\ddot{w} \tag{6}$$

$$-\frac{f^2}{k}(\dot{u}^{\mathrm{f}}-\dot{u})-f\frac{\vartheta p}{\vartheta x}=f\rho_{\mathrm{f}}\ddot{u}^{\mathrm{f}} \tag{7}$$

$$-\frac{f^2}{k}(\dot{w}^{\mathrm{f}}-\dot{w})-f\frac{\vartheta p}{\vartheta z}=f\rho_{\mathrm{f}}\ddot{w}^{\mathrm{f}} \tag{8}$$

$$f\left(\frac{\vartheta\dot{u}^{\mathrm{f}}}{\vartheta x}+\frac{\vartheta\dot{w}^{\mathrm{f}}}{\vartheta z}\right)+(1-f)\left(\frac{\vartheta\dot{u}}{\vartheta x}+\frac{\vartheta\dot{w}}{\vartheta z}\right)=-\frac{f}{\beta}\dot{p} \tag{9}$$

where Eqs. (5) and (6) describe the motion of the solid as affected by the motion of the fluid and Eqs. (7) and (8) describe Darcy's law of the fluid flow as affected by the motion of the solid. It should be noted that in the original formulation, Biot (1956) also included apparent inertia terms to describe the dynamic interaction between the two constituents. However, the apparent mass density, difficult to assess theoretically or experimentally, is often omitted by most researchers as explained in detail by Mei and Foda (1981). In the above Eqs. (5)–(9), τ_x and τ_z are the normal effective stresses of the solid along the x and z coordinates, respectively, τ_{xz} is the effective shearing stress of the solid in the x–z plane, p is the fluid pressure, u and w are the solid displacement components along the x and z directions, respectively, relative to the bedrock, u^{f} and w^{f} are the corresponding displacement components of the fluid and dots indicate differentiation with respect to time t. Furthermore, f is the porosity, ρ_{s} and ρ_{f} are the actual mass densities of the solid and the fluid, respectively, k denotes the coefficient of permeability, and β is the bulk modulus of the fully saturating fluid. In general, all functions of the system depend on x, z and t.

For the two-dimensional, plane strain conditions examined herein and with the assumption that Hooke's law with hysteretic damping relates stresses and strains of the solid skeleton one has

$$\tau_x=(\lambda^*+2G^*)\frac{\vartheta u}{\vartheta x}+\lambda^*\frac{\vartheta w}{\vartheta z} \tag{10}$$

$$\tau_{xz}=G^*\left(\frac{\vartheta u}{\vartheta z}+\frac{\vartheta w}{\vartheta x}\right) \tag{11}$$

$$\tau_z=(\lambda^*+2G^*)\frac{\vartheta w}{\vartheta z}+\lambda^*\frac{\vartheta u}{\vartheta x} \tag{12}$$

in which G^* and λ^* are the complex-valued Lamé elastic constants given by

$$G^*=G(1+\mathrm{i}\delta),\quad \mathrm{i}=\sqrt{-1} \tag{13}$$

$$\lambda^*=\frac{2v}{1-2v}G^* \tag{14}$$

with v being the Poisson's ratio, G the constant shear modulus and δ the constant material damping factor.

Adding Eqs. (5) and (7) and Eqs. (6) and (8), respectively, and using Eqs. (10)–(12) in the resulting expressions one has

$$(\lambda^* + 2G^*)\frac{\vartheta^2 u}{\vartheta x^2} + (\lambda^* + G^*)\frac{\vartheta^2 w}{\vartheta x\,\vartheta z} + G^*\frac{\vartheta^2 u}{\vartheta z^2} - \frac{\vartheta p}{\vartheta x} = (1-f)\rho_s\ddot{u} + f\rho_f\ddot{u}^f \tag{15}$$

$$(\lambda^* + 2G^*)\frac{\vartheta^2 w}{\vartheta z^2} + (\lambda^* + G^*)\frac{\vartheta^2 u}{\vartheta x\,\vartheta z} + G^*\frac{\vartheta^2 w}{\vartheta x^2} - \frac{\vartheta p}{\vartheta z} = (1-f)\rho_s\ddot{w} + f\rho_f\ddot{w}^f \tag{16}$$

Thus, the system of Eqs. (5)–(12) can be replaced by the equivalent one of the five Eqs. (7)–(9), (15) and (16) with five unknowns u, u^f, w, w^f and p. The method of solution of the problem considered herein is based on the theory of Mei and Foda (1981), according to which the total field of a poroelastic problem obeying Biot's (1956) theory can be approximated by the superposition of (i) an elastodynamic problem with modified elastic constants and mass density for the whole domain (the outer approximation) and (ii) a diffusion problem for the pore fluid pressure confined to a thin boundary layer at the free boundaries of the domain (the boundary layer correction). This implies that any total response function $\phi = \phi(x,z,t)$ of the system has the form

$$\phi(x,z,t) = \phi^o(x,z,t) + \phi^b(x,z,t) \tag{17}$$

where the outer approximation and the boundary layer correction functions are distinguished by the superscripts o and b, respectively.

Provided that the applied load is given by Eq. (1) and since the layer properties are independent of the spatial coordinates, any response functions $\phi^o(x,z,t)$, $\phi^b(x,z,t)$ and $\phi(x,z,t)$ of the linear system may be expressed as a linear combination of corresponding harmonic functions in the form

$$\phi^o(x,z,t) = \mathrm{Re}\sum_{n=-\infty}^{\infty} \Phi_n^o(z)\,\mathrm{e}^{\mathrm{i}\lambda_n(x-ct)} \tag{18a}$$

$$\phi^b(x,z,t) = \mathrm{Re}\sum_{n=-\infty}^{\infty} \Phi_n^b(z)\,\mathrm{e}^{\mathrm{i}\lambda_n(x-ct)} \tag{18b}$$

$$\phi(x,z,t) = \mathrm{Re}\sum_{n=-\infty}^{\infty} \Phi_n(z)\,\mathrm{e}^{\mathrm{i}\lambda_n(x-ct)} \tag{18c}$$

with

$$\Phi_n(z) = \Phi_n^o(z) + \Phi_n^b(z) \tag{19}$$

in which, for example, $\Phi_n^o(z) = \Phi_n^o$ represents the dependence of the outer approximation response $\phi^o(x,z,t)$ on z only, for the nth harmonic.

3.1. The outer approximation problem

On the assumption that the dimensionless quantity R

$$R = \frac{f\lambda_n c H^2}{Gk} \gg 1 \tag{20}$$

Mei and Foda (1981) argued that the outer region moves as a whole like an undrained system. It should be noted that the quantity $\lambda_n c$ in Eq. (20) represents the parameter of frequency in the domain of Fourier expansion considered. Thus, one has

$$w^o = (w^f)^o, \quad u^o = (u^f)^o \tag{21}$$

On the basis of Eq. (21), one can obtain from Eq. (9), after integration with respect to time, the following expression for the associated pore fluid pressure

$$p^{o} = -\frac{\beta}{f}\left(\frac{\vartheta u^{o}}{\vartheta x} + \frac{\vartheta w^{o}}{\vartheta z}\right) \tag{22}$$

Consequently, on making use of Eqs. (21) and (22) into Eqs. (15) and (16) and integrating the resulting expressions with respect to time, one receives

$$G^{*}\left(\frac{\vartheta^{2}u^{o}}{\vartheta x^{2}} + \frac{\vartheta^{2}u^{o}}{\vartheta z^{2}}\right) + (\lambda^{*} + G^{*} + \beta/f)\left(\frac{\vartheta^{2}u^{o}}{\vartheta x^{2}} + \frac{\vartheta^{2}w^{o}}{\vartheta x\,\vartheta z}\right) = [(1-f)\rho_{s} + f\rho_{f}]\ddot{u}^{o} \tag{23}$$

$$G^{*}\left(\frac{\vartheta^{2}w^{o}}{\vartheta x^{2}} + \frac{\vartheta^{2}w^{o}}{\vartheta z^{2}}\right) + (\lambda^{*} + G^{*} + \beta/f)\left(\frac{\vartheta^{2}w^{o}}{\vartheta z^{2}} + \frac{\vartheta^{2}u^{o}}{\vartheta x\,\vartheta z}\right) = [(1-f)\rho_{s} + f\rho_{f}]\ddot{w}^{o} \tag{24}$$

It is observed that Eqs. (23) and (24) are the same as in classical elastodynamics for a simple phase medium but with new equivalent elastic constants and mass density given by

$$G_{e}^{*} = G^{*} \tag{25a}$$

$$\lambda_{e}^{*} = \lambda^{*} + \beta/f \tag{25b}$$

$$\rho_{e} = (1-f)\rho_{s} + f\rho_{f} \tag{25c}$$

Thus, the outer region problem is essentially reduced to a usual elastodynamic problem with a free surface, which can be easily solved to determine w^{o} and u^{o}. Then, the pore fluid pressure is determined by Eq. (22), which simply states that in the undrained outer region the pore pressure is related to the dilatation of the solid matrix. It should be noted that the part of response due to the outer approximation solution does not depend on the permeability k of the poroelastic medium.

3.2. The boundary layer correction

According to the theory of Mei and Foda (1981), within a thin boundary layer near the free surface of the medium, for any functions one has $\vartheta/\vartheta z \gg \vartheta/\vartheta x$, which implies that $\vartheta\tau_{xz}^{b}/\vartheta x = 0$ and the dominant term is $\vartheta^{2}w^{b}/\vartheta z^{2}$ relative to which the inertia terms are negligible. Based on these assumptions, Eqs. (6), (8), (9) and (12) can be written as

$$\frac{\vartheta\tau_{z}^{b}}{\vartheta z} + \frac{f^{2}}{k}((\dot{w}^{f})^{b} - \dot{w}^{b}) - (1-f)\frac{\vartheta p^{b}}{\vartheta z} = 0 \tag{26}$$

$$-\frac{f^{2}}{k}((\dot{w}^{f})^{b} - \dot{w}^{b}) = f\frac{\vartheta p^{b}}{\vartheta z} \tag{27}$$

$$f\frac{\vartheta}{\vartheta z}((\dot{w}^{f})^{b} - \dot{w}^{b}) + \frac{\vartheta\dot{w}^{b}}{\vartheta z} = -\frac{f}{\beta}\dot{p}^{b} \tag{28}$$

$$\tau_{z}^{b} = (\lambda^{*} + 2G^{*})\frac{\vartheta w^{b}}{\vartheta z} \tag{29}$$

where Eq. (27) is the static form of Darcy's law. Thus, the system of Eqs. (26)–(29) can be solved to determine w^{b}, $(w^{f})^{b}$, τ_{z}^{b} and p^{b} in the boundary layer.

Adding Eqs. (26) and (27) one receives $\vartheta\tau_z^{\mathrm{b}}/\vartheta z = \vartheta p^{\mathrm{b}}/\vartheta z$, which after integration with respect to z (with the integration constant equal to zero since both τ_z^{b} and p^{b} vanish beyond the limit of the boundary layer) yields

$$\tau_z^{\mathrm{b}} = p^{\mathrm{b}} \tag{30}$$

Consequently, after differentiation of Eq. (27) with respect to z, substitution of the resulting expression into Eq. (28) and use of Eqs. (29) and (30), one receives

$$k\frac{\vartheta^2 p^{\mathrm{b}}}{\vartheta^2 z} - D\dot{p}^{\mathrm{b}} = 0 \quad \text{with } D = \frac{f}{\beta} + \frac{1}{\lambda^* + 2G^*} \tag{31}$$

which is a heat diffusion equation and can be easily solved. Eq. (31) is the governing equation of the boundary layer for the pore fluid pressure p^{b}. This boundary layer formulation is only valid if

$$H/d \gg 1 \tag{32}$$

in which d is the boundary layer thickness.

4. Solution of the governing equations

4.1. Boundary conditions

The solution of the governing equations for the whole domain (outer region and boundary layer) can be found by employing the following four boundary conditions:

$$\text{at the bottom } (z = H): \quad w = w^{\mathrm{o}} = 0, \quad u = u^{\mathrm{o}} = 0 \tag{33a}$$

$$\text{at the surface } (z = 0): \quad \tau_{xz} = \tau_{xz}^{\mathrm{o}} = 0, \quad \tau_z = \tau_z^{\mathrm{o}} + \tau_z^{\mathrm{b}} = F \tag{33b}$$

or in terms of the corresponding harmonics, on account of Eqs. (17) and (18), by

$$\text{at the bottom } (z = H): \quad W_n^{\mathrm{o}} = 0, \quad U_n^{\mathrm{o}} = 0 \tag{34a}$$

$$\text{at the surface } (z = 0): \quad T_{xz,n}^{\mathrm{o}} = 0, \quad T_{z,n}^{\mathrm{o}} + T_{z,n}^{\mathrm{b}} = F_n \tag{34b}$$

In addition, the governing equations of the boundary layer can be solved subject to the boundary conditions

$$\text{at the bottom of the boundary layer } (z = d): \quad p^{\mathrm{b}} = 0 \tag{35a}$$

$$\text{at the surface } (z = 0): \quad p = p^{\mathrm{o}} + p^{\mathrm{b}} = 0 \tag{35b}$$

or in terms of the corresponding harmonics

$$\text{at the bottom of the boundary layer } (z = d): \quad P_n^{\mathrm{b}} = 0 \tag{36a}$$

$$\text{at the surface } (z = 0): \quad P_n^{\mathrm{o}} + P_n^{\mathrm{b}} = 0 \tag{36b}$$

4.2. Solution for the outer approximation

It is noticeable that, in the Mei and Foda's (1981) theory, the boundary layer does not affect the traction of the free surface so that the outer approximation may be solved first by the usual methods of elasticity

theory. Thus, on making use of general expression (18a) and Eq. (25), the system of the governing Eqs. (23) and (24) for the two displacement responses of the soil layer in the outer domain reads

$$a_1(W_n^{\mathrm{o}})'' + b_1 W_n^{\mathrm{o}} + d_1(U_n^{\mathrm{o}})' = 0 \tag{37}$$

$$a_2(U_n^{\mathrm{o}})'' + b_2 U_n^{\mathrm{o}} + d_2(W_n^{\mathrm{o}})' = 0 \tag{38}$$

in which, a prime denotes differentiation with respect to z and the coefficients a_1, b_1, d_1, a_2, b_2 and d_2 are given by the following expressions

$$\begin{aligned} a_1 &= \lambda_{\mathrm{e}}^* + 2G^* \\ b_1 &= -G^*\lambda_n^2 + \rho_{\mathrm{e}}\lambda_n^2 c \\ d_1 &= (\lambda_{\mathrm{e}}^* + G^*)\mathrm{i}\lambda_n \\ a_2 &= G^* \\ b_2 &= -(\lambda_{\mathrm{e}}^* + 2G^*)\lambda_n^2 + \rho_{\mathrm{e}}\lambda_n^2 c^2 \\ d_2 &= d_1 \end{aligned} \tag{39}$$

Assuming solutions for the two displacements of the form

$$W_n^{\mathrm{o}} = A\,\mathrm{e}^{qz}, \quad U_n^{\mathrm{o}} = B\,\mathrm{e}^{qz} \tag{40}$$

the general solution of the system of Eqs. (37) and (38) is of the form

$$W_n^{\mathrm{o}} = A_{1n}\,\mathrm{e}^{q_1 z} + A_{2n}\,\mathrm{e}^{q_2 z} + A_{3n}\,\mathrm{e}^{q_3 z} + A_{4n}\,\mathrm{e}^{q_4 z} \tag{41}$$

$$U_n^{\mathrm{o}} = B_{1n}\,\mathrm{e}^{q_1 z} + B_{2n}\,\mathrm{e}^{q_2 z} + B_{3n}\,\mathrm{e}^{q_3 z} + B_{4n}\,\mathrm{e}^{q_4 z} \tag{42}$$

where

$$B_{\kappa n} = r_{\kappa n} A_{\kappa n}, \quad r_{\kappa n} = -\frac{a_1 q_\kappa^2 + b_1}{d_1 q_\kappa} \tag{43}$$

and q_κ ($\kappa = 1$–4) are the roots of the fourth-degree characteristic equation of the system of Eqs. (37) and (38) given by

$$\det \begin{vmatrix} a_1 q^2 + b_1 & d_1 q \\ d_2 q & a_2 q^2 + b_2 \end{vmatrix} = 0 \tag{44}$$

Furthermore, on account of Eq. (18a) the expressions of the harmonics for the effective shearing stress, the effective vertical stress and the pore water pressure (based on Eqs. (11), (12) and (22), respectively) are given by

$$T_{xz,n}^{\mathrm{o}} = G^*((U_n^{\mathrm{o}})' + \mathrm{i}\lambda_n W_n^{\mathrm{o}}) \tag{45}$$

$$T_{z,n}^{\mathrm{o}} = (\lambda^* + 2G^*)(W_n^{\mathrm{o}})' + \lambda^*(\mathrm{i}\lambda_n)U_n^{\mathrm{o}} \tag{46}$$

$$P_n^{\mathrm{o}} = -\frac{\beta}{f}(\mathrm{i}\lambda_n U_n^{\mathrm{o}} + (W_n^{\mathrm{o}})') \tag{47}$$

The four unknown integration constants $A_{\kappa n}$ of Eqs. (41) and (42) may now be determined by employing the boundary conditions given by Eqs. (34a) and (34b) with the second of Eq. (34b), in view of Eqs. (30) and (36b), receiving the form

$$T_{z,n}^{\mathrm{b}}(z=0) = P_n^{\mathrm{b}}(z=0) = -P_n^{\mathrm{o}}(z=0) \tag{48}$$

Thus, one can write down the following system of equations for the determination of the integration constants $A_{\kappa n}$:

$$\begin{aligned}
&A_{1n}\mathrm{e}^{q_1 H} + A_{2n}\mathrm{e}^{q_2 H} + A_{3n}\mathrm{e}^{q_3 H} + A_{4n}\mathrm{e}^{q_4 H} = 0\\
&r_{1n}A_{1n}\mathrm{e}^{q_1 H} + r_{2n}A_{2n}\mathrm{e}^{q_2 H} + r_{3n}A_{3n}\mathrm{e}^{q_3 H} + r_{4n}A_{4n}\mathrm{e}^{q_4 H} = 0\\
&(q_1 r_{1n}A_{1n} + q_2 r_{2n}A_{2n} + q_3 r_{3n}A_{3n} + q_4 r_{4n}A_{4n}) + \mathrm{i}\lambda_n(A_{1n} + A_{2n} + A_{3n} + A_{4n}) = 0\\
&(\lambda^* + 2G^* + \beta/f)(q_1 A_{1n} + q_2 A_{2n} + q_3 A_{3n} + q_4 A_{4n}) + (\lambda^* + \beta/f)\mathrm{i}\lambda_n(r_{1n}A_{1n} + r_{2n}A_{2n} + r_{3n}A_{3n} + r_{4n}A_{4n}) = F_n
\end{aligned} \tag{49}$$

With the integration constants A_{1n}, A_{2n}, A_{3n} and A_{4n} known, any response associated with the outer approximation can be estimated with the aid of Eqs. (41), (42), (46) and (47), for the nth harmonic F_n.

4.3. Solution for the boundary layer correction

On the basis of Eq. (18b), the governing equation of the boundary layer for the pore fluid pressure, Eq. (31), can be written as

$$(P_n^{\mathrm{b}})'' - \frac{(-\mathrm{i}\lambda_n c)}{k} D P_n^{\mathrm{b}} = 0 \tag{50}$$

Following the argument of Mei and Foda (1981), Eq. (50) implies that the boundary layer thickness for the nth harmonic is

$$d_n = \sqrt{\frac{k}{\lambda_n c}}\sqrt{\frac{1}{D}} \tag{51}$$

For the solution of Eq. (50) one assumes that

$$P_n^{\mathrm{b}}(z) = \Gamma \mathrm{e}^{sz} \tag{52}$$

where s has to be determined. Thus, Eq. (50), with the aid of Eqs. (51) and (52) becomes

$$\Gamma\left(s^2 + \frac{1}{d_n^2}\mathrm{i}\right) = 0 \tag{53}$$

which can be solved for the two roots

$$s_{1,2} = \pm\frac{1-\mathrm{i}}{d_n\sqrt{2}} \tag{54}$$

Hence, the general solution of Eq. (50), in view of Eq. (52) is given by

$$P_n^{\mathrm{b}}(z) = \Gamma_{1n}\mathrm{e}^{s_1 z} + \Gamma_{2n}\mathrm{e}^{s_2 z} \tag{55}$$

The two arbitrary constants Γ_1 and Γ_2 in Eq. (55) may be related to the known pore fluid pressure of the outer field, P_n^{o}, by employing the boundary conditions given by Eq. (36). Thus, one receives

$$\Gamma_{1n} = -P_n^{\mathrm{o}}(z=0)\frac{1}{1-\mathrm{e}^{\sqrt{2}(1-\mathrm{i})}}, \quad \Gamma_{2n} = +P_n^{\mathrm{o}}(z=0)\frac{\mathrm{e}^{\sqrt{2}(1-\mathrm{i})}}{1-\mathrm{e}^{\sqrt{2}(1-\mathrm{i})}} \tag{56}$$

4.4. Outline of response analysis procedure

It has already been mentioned through Eqs. (17)–(19) that the total response of the system is given as the sum of the outer approximation response and the boundary layer correction response, if any. Thus, in view

of the equations found in the previous sections, the outline of the response analysis procedure for the total vertical displacement, pore fluid pressure and vertical effective stress in the whole domain can be summarized as follows:

1. Solve the system of Eq. (49) for A_{1n}, A_{2n}, A_{3n} and A_{4n}.
2. Calculate W_n^{o}, U_n^{o}, $T_{z,n}^{\mathrm{o}}$ and P_n^{o} from Eqs. (41), (42), (46) and (48), respectively.
3. Determine Γ_{1n} and Γ_{2n} from Eq. (55) and P_n^{b} from Eq. (54). The latter, after elaboration, yields

$$P_n^{\mathrm{b}}(z) = P_n^{\mathrm{b}} = P_n^{\mathrm{o}}(z=0)[-\mathrm{e}^{sz} + \mathrm{e}^{\sqrt{2}(1-\mathrm{i})}\,\mathrm{e}^{-sz}]/(1-\mathrm{e}^{\sqrt{2}(1-\mathrm{i})}) \tag{57}$$

4. Determine $T_{z,n}^{\mathrm{b}}$ from Eq. (30).
5. Determine $W_n^{\mathrm{b}}(z) = W_n^{\mathrm{b}}$ from Eq. (29) after integration with respect to z. The integration constant can be found by employing the condition that $W_n^{\mathrm{b}}(z=d_n) = 0$. Thus, one has

$$W_n^{\mathrm{b}} = P_n^{\mathrm{o}}(z=0)\frac{\sqrt{2}d_n}{1-\mathrm{i}}\left[-\mathrm{e}^{\frac{1-\mathrm{i}}{\sqrt{2}d_n}z} - \mathrm{e}^{\sqrt{2}(1-\mathrm{i})}\,\mathrm{e}^{-\frac{1-\mathrm{i}}{\sqrt{2}d_n}z} + 2\mathrm{e}^{\frac{1-\mathrm{i}}{\sqrt{2}}}\right]\Big/[(\lambda^* + 2G^*)(1-\mathrm{e}^{\sqrt{2}(1-\mathrm{i})})] \tag{58}$$

6. Finally, on the basis of the general expressions (17)–(19), the expressions of the applied load given by Eqs. (2)–(4) and the aforementioned steps, the resulting expressions for the relative vertical solid displacement, pore fluid pressure and effective vertical solid stress can be written in the form

$$\begin{aligned}
w(x,z,t) &= \mathrm{Re}\sum_0^{2048}(W_n^{\mathrm{o}} + W_n^{\mathrm{b}})\,\mathrm{e}^{\mathrm{i}\lambda_n(x-ct)} \quad \text{for } 0 \leqslant z \leqslant d_n \\
w(x,z,t) &= \mathrm{Re}\sum_0^{2048} W_n^{\mathrm{o}}\,\mathrm{e}^{\mathrm{i}\lambda_n(x-ct)} \quad \text{for } d_n \leqslant z \leqslant H \\
p(x,z,t) &= \mathrm{Re}\sum_0^{2048}(P_n^{\mathrm{o}} + P_n^{\mathrm{b}})\,\mathrm{e}^{\mathrm{i}\lambda_n(x-ct)} \quad \text{for } 0 \leqslant z \leqslant d_n \\
p(x,z,t) &= \mathrm{Re}\sum_0^{2048} P_n^{\mathrm{o}}\,\mathrm{e}^{\mathrm{i}\lambda_n(x-ct)} \quad \text{for } d_n \leqslant z \leqslant H \\
\tau_{z,n}(x,z,t) &= \mathrm{Re}\sum_0^{2048}(T_{z,n}^{\mathrm{o}} + T_{z,n}^{\mathrm{b}})\,\mathrm{e}^{\mathrm{i}\lambda_n(x-ct)} \quad \text{for } 0 \leqslant z \leqslant d_n \\
\tau_{z,n}(x,z,t) &= \mathrm{Re}\sum_0^{2048} T_{z,n}^{\mathrm{o}}\,\mathrm{e}^{\mathrm{i}\lambda_n(x-ct)} \quad \text{for } d_n \leqslant z \leqslant H
\end{aligned} \tag{59}$$

The special case of the harmonic for $n = 0$ will be discussed in detail in the next section.

4.5. The special case of harmonic for $n = 0$

One can see that for the case of $n = 0$, Eq. (4) implies that $\lambda_{n=0} = 0$, which leads to zero values for the coefficients b_1, d_1, b_2, and c_2 of Eq. (39), thus rendering the solution of Eq. (49) impossible. Moreover, the value of $\lambda_{n=0} = 0$ gives an infinite value of boundary layer depth through Eq. (51). This problem is solved by calculating separately the term $\Phi_{n=0}(z)$ for any response function.

On substituting the value of $\lambda_{n=0} = 0$ into the governing equations of both the outer approximation and the boundary layer correction, Eqs. (37), (38) and (50), respectively, and employing the boundary conditions of the problem it is easily shown that

$$
\begin{aligned}
W^{\mathrm{o}}_{n=0}(z) &= \frac{\ell}{L} F \frac{1}{\lambda^* + 2G^* + \beta/f}(z-H) \\
W^{\mathrm{b}}_{n=0}(z) &= \frac{\ell}{L} F \frac{1}{\lambda^* + 2G^* + \beta/f} \frac{\beta/f}{\lambda^* + 2G^*}(z-H) \\
U_{n=0}(z) &= 0 \\
P^{\mathrm{o}}_{n=0}(z) &= -\frac{\ell}{L} F \frac{\beta/f}{\lambda^* + 2G + \beta/f} \\
P^{\mathrm{b}}_{n=0}(z) &= +\frac{\ell}{L} F \frac{\beta/f}{\lambda^* + 2G^* + \beta/f} \\
P_{n=0}(z) &= 0 \\
T^{\mathrm{o}}_{z,n=0}(z) &= \frac{\ell}{L} F \frac{\lambda^* + 2G^*}{\lambda^* + 2G^* + \beta/f} \\
T^{\mathrm{b}}_{z,n=0}(z) &= \frac{\ell}{L} F \frac{\beta/f}{\lambda^* + 2G^* + \beta/f} \\
T_{z,n=0}(z) &= \frac{\ell}{L} F
\end{aligned}
\tag{60}
$$

It is worth noting that for the case of the frequency factor $\lambda_{n=0} = 0$, Eq. (50) with its original form given by Eq. (31), simulates the Terzaqhi equation for one-dimensional consolidation. In such a case, since the only time scale is the diffusion time, the boundary layer is the entire soil depth (Mei and Foda, 1981), i.e., $d_{n=0} = H$.

5. Numerical results and discussion

As an application of the approximate solution procedure presented in this work, as well as for the sake of comparison of the results obtained by this solution procedure with those found by the exact solution procedure in Theodorakopoulos (2003), the problem of a single poroelastic soil layer of depth 18 m, extending to infinity in the lateral directions, resting on an impervious bedrock and subjected to a surface vertical strip load moving at a constant velocity c, was investigated. The numerical results of this section have been obtained on the basis of the numerical values of the material coefficients given in Table 1. The value of bulk modulus $\beta = 2.45 \times 10^9$ N/m^2 corresponds to the compressibility of pure water for full saturation, whereas the values of permeability $k = 10^{-9}$ m^3 s/kg $= 10^{-5}$ m/s (fine material) and $k = 10^{-7}$ m^3 s/kg $= 10^{-3}$ m/s (coarse material) are typical values for the soil medium of the problem considered. The main physical quantities of interest in this investigation are the vertical displacement of the solid, $w(x,z,t)$, the pore water pressure, $p(x,z,t)$, and the vertical effective stress, $\tau_z(x,z,t)$. The variation of these quantities

Table 1
Numerical values of coefficients for water fully saturated poroelastic material

Shear modulus of solid	$G = 10^8$–0.2×10^8 N/m^2
Bulk modulus of water	$\beta = 2.45 \times 10^9$ N/m^2
Poisson's ratio	$v = 0.35$
Solid density	$\rho_s = 1816$ kg/m^3
Water density	$\rho_f = 1000$ kg/m^3
Porosity	$f = 0.40$
Permeability	$k = 10^{-9}$–10^{-7} m^3 s/kg $= 10^{-5}$–10^{-3} m/s
Coefficient of material damping	$\delta = 0.1$

with respect to the velocity c, permeability k, porosity f and shear modulus of solid G, according to the approximate theory of Mei and Foda (1981) and consequently the accuracy of the present method against the exact one, are evaluated in this section.

In what follows, the time $t = 0$ corresponds to the instant at which the center of the applied load passes the point with $x = 0$ and $z = 0$, at which the maximum value of any response function occurs. Furthermore, it is clear that any response pattern underneath the load, at any time t, will appear to be the same for an observer traveling with velocity c.

5.1. The boundary layer correction contribution

For the range of values of material properties and load velocities used in this work, the validity of the basic assumptions of the theory of Mei and Foda (1981) as applied to the problem of this paper is investigated firstly. Mention has already been made that the solution presented herein must satisfy the expressions given by Eqs. (20) and (32). Table 2 shows the values of the quantities $R_{n=1}$, $d_{n=1}$ and $H/d_{n=1}$ for various combinations of permeability, shear modulus and load speed. It should be noted that, due to the nature of Eqs. (20) and (32), for the harmonic with $n = 1$ the quantities $R_{n=1}$ and $d_{n=1}$ correspond to minimum value of R and maximum layer depth d_n, respectively, for the total number of harmonics. Thus, one can observe that for low permeability, both expressions (20) and (32) give values well above unity, whereas for high permeability both the $R_{n=1}$ and the ratio $H/d_{n=1}$ are hardly greater than unity, especially for high shear modulus and low load velocity. From Table 2, it is also evident, as expected (Mei and Foda, 1981), that the boundary layer thickness decreases with decreasing permeability, decreasing shear modulus and increasing frequency (with $\lambda_n c$ being the frequency factor).

The effect of adding the contribution of the boundary layer correction to the outer approximation response is shown in Figs. 2–4 for the vertical solid displacement, porewater pressure and solid vertical effective stress, respectively. As mentioned in a previous section, any response of the outer approximation solution is independent of the value of k. More specifically, Fig. 2(a) and (b) shows the vertical distribution of both the outer approximation and total response of the maximum vertical displacement for two different values of permeability k, $G = 10^8$ N/m^2 and a specific value of load velocity in each figure. One can see that for both values of load velocity, the effect of boundary layer correction is a small percentage of the total displacement response and increases with increasing permeability. Indeed, for $k = 10^{-9}$ m^3 s/kg $= 10^{-5}$ m/s the outer approximation response is of about 94% of the total response at the free surface and in this case the boundary layer correction can be neglected for engineering purposes. More details about this will be given in the following section. It should be noted that the discrepancy between the outer approximation and the total response over the whole soil layer depth is due to harmonic for $n = 0$, for which $d_{n=0} = H$, as mentioned in a previous section.

Fig. 3(a) and (b) shows the vertical variation of both the outer approximation and the total response concerning the pore water pressure, again for two different values of permeability k, $G = 10^8$ N/m^2 and a

Table 2
Maximum value of boundary layer depth from Eq. (51) with $n = 1$, for various combinations of k, c and G

G (N/m^2)	$k = 10^{-9}$ m^3 s/kg $= 10^{-5}$ m/s, $f = 0.40$						$k = 10^{-7}$ m^3 s/kg $= 10^{-3}$ m/s, $f = 0.40$					
	$c = 20$ m/s			$c = 100$ m/s			$c = 20$ m/s			$c = 100$ m/s		
	$R_{n=1}$	$d_{n=1}$ (m)	$H/d_{n=1}$	$R_{n=1}$	$d_{n=1}$ (m)	$H/d_{n=1}$	$R_{n=1}$	$d_{n=1}$ (m)	$H/d_{n=1}$	$R_{n=1}$	$d_{n=1}$ (m)	$H/d_{n=1}$
10^8	400	1.148	16	1990	0.513	35	4.0	11.48	1.6	19.9	5.13	3.5
0.50×10^8	790	0.825	22	3980	0.369	49	7.9	8.25	2.2	39.8	3.69	4.9
0.35×10^8	1140	0.694	26	5670	0.310	58	11.4	6.94	2.6	56.7	3.10	5.8
0.20×10^8	1980	0.528	34	9930	0.236	76	19.8	5.28	3.4	99.3	2.36	7.6

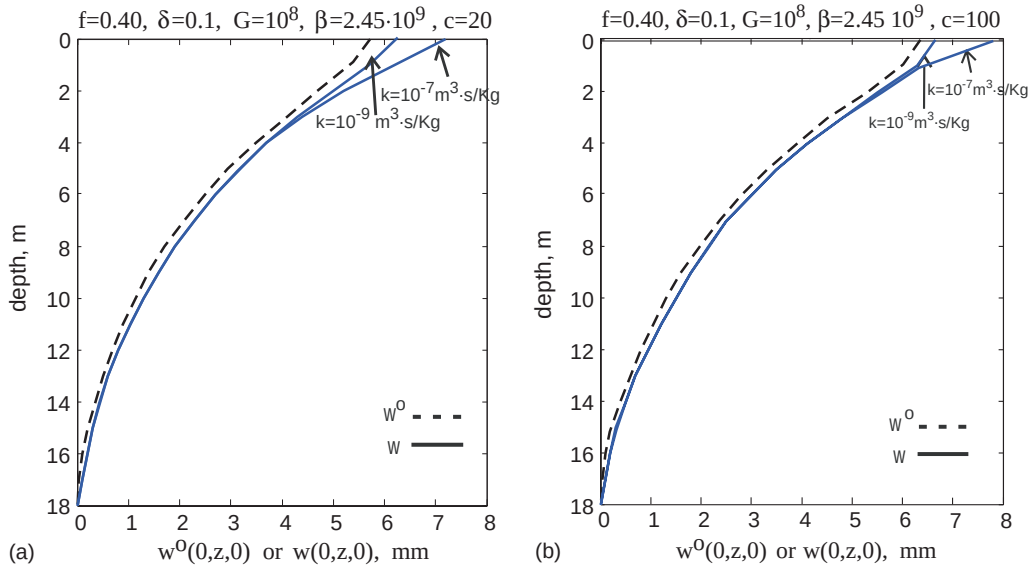

Fig. 2. Effect of the boundary layer correction on maximum solid vertical displacement versus depth for $c = 20$ m/s (a) and $c = 100$ m/s (b).

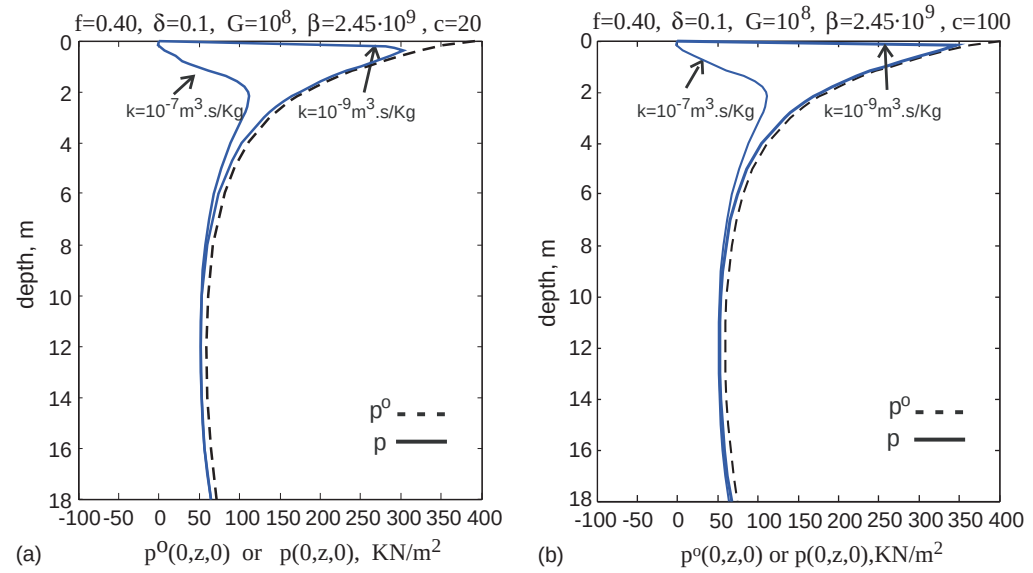

Fig. 3. Effect of the boundary layer correction on the profile of the porewater pressure for $c = 20$ m/s (a) and $c = 100$ m/s (b).

specific value of load velocity in each figure. It can be seen that, for both values of velocity c, in the case of low permeability ($k = 10^{-9}$ m^3 s/kg $= 10^{-5}$ m/s) the total pore water pressure $p(0, z, 0)$ increases rapidly with depth near the free surface and then diminishes gradually up to a constant value. On the other hand, for $k = 10^{-7}$ m^3 s/kg $= 10^{-3}$ m/s, which implies a boundary layer depth not small compared to the total layer

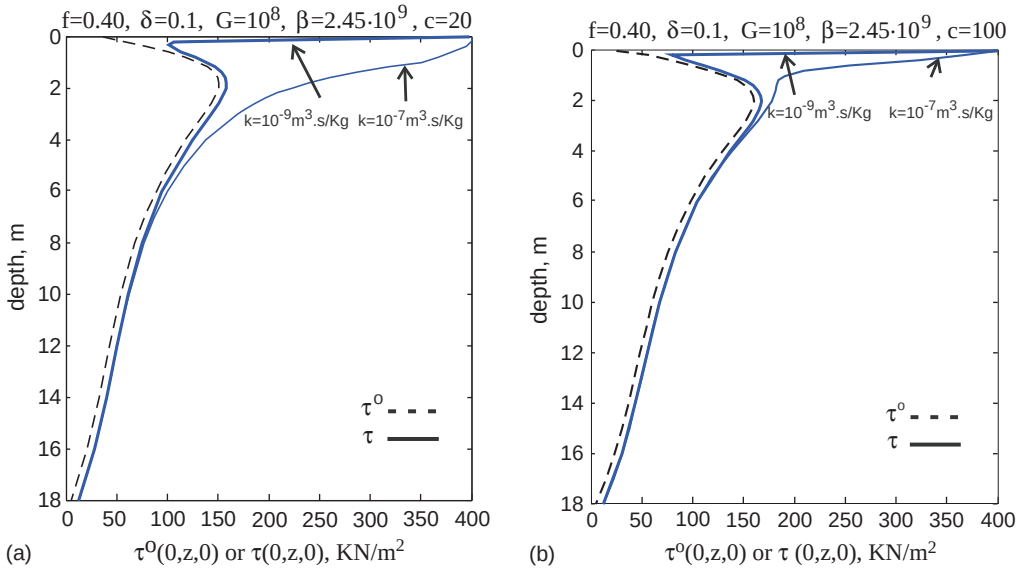

Fig. 4. Effect of the boundary layer correction on the profile of maximum effective vertical stress for $c = 20$ m/s (a) and $c = 100$ m/s (b).

depth H (see Table 2), the variation of the total pore water pressure is similar but with a lower maximum value near the surface than in the previous case. This lower maximum value of the pore pressure near the surface in the case of $k = 10^{-7}$ m^3 s/kg $= 10^{-3}$ m/s is due to the fact that for a more permeable poroelastic soil the water is more free to squeeze in and out. It should be also mentioned here that the pore water pressure distribution in Fig. 3(a) and (b) is similar to the one given in Foda and Mei (1983) for the case of Rayleigh waves in a poroelastic half-space. As far as the distribution of the vertical effective stress τ_z is concerned, one can see from Fig. 4(a) and (b) that the variation of $\tau_z(0, z, 0)$ versus z for the same values of the parameters as in Fig. 3(a) and (b), follows similar but opposite with respect to k patterns to those observed for $p(0, z, 0)$, starting from 400 kN/m^2 at the surface, since both the solid and fluid constituents share the applied load at any depth.

Referring back to Fig. 3(a) and (b), it can be observed that, for fine materials ($k = 10^{-9}$ m^3 s/kg $= 10^{-5}$ m/s), the vertical pore water distributions given by the outer approximation solution and the total solution are nearly the same in any respect except in the part near the free surface where the effect of the boundary layer correction gives the expected distribution, that is, zero pore water pressure at the free surface (Eq. (35b)). It is also of interest to note that the value of p^o at the surface, which has an absolute value equal to the vertical effective stress component due to the boundary layer correction, τ_z^b, approaches the value of the applied stress $F = 400$ kN/m^2 (Fig. 3(a) and (b)), whereas the value of τ_z^o is very close to zero (Fig. 4(a) and (b)). This is due to the high value of water compressibility $\beta = 2.45 \times 10^9$ N/m^2 used here as compared to the shear modulus $G = 10^8$ N/m^2 ($G/\beta = 0.041$), which affects the values of the coefficients of Eqs. (47) and (46) for P_n^o and $T_{z,n}^o$, respectively. For a rather compressible fluid with $\beta = 10^8$ N/m^2 ($G/\beta = 1.0$), the sharing of the applied load between τ_z^o and τ_z^b ($= -p^o$) changes, thus, reducing the values of p^o at the surface to 176 and 183 kN/m^2 for $c = 20$ and 100 m/s, respectively.

5.2. Comparison between approximate method and exact solution

Fig. 5(a)–(c) shows the variation with depth of the vertical displacement, porewater pressure and solid vertical effective stress, respectively, according to both the present approximate method and the exact

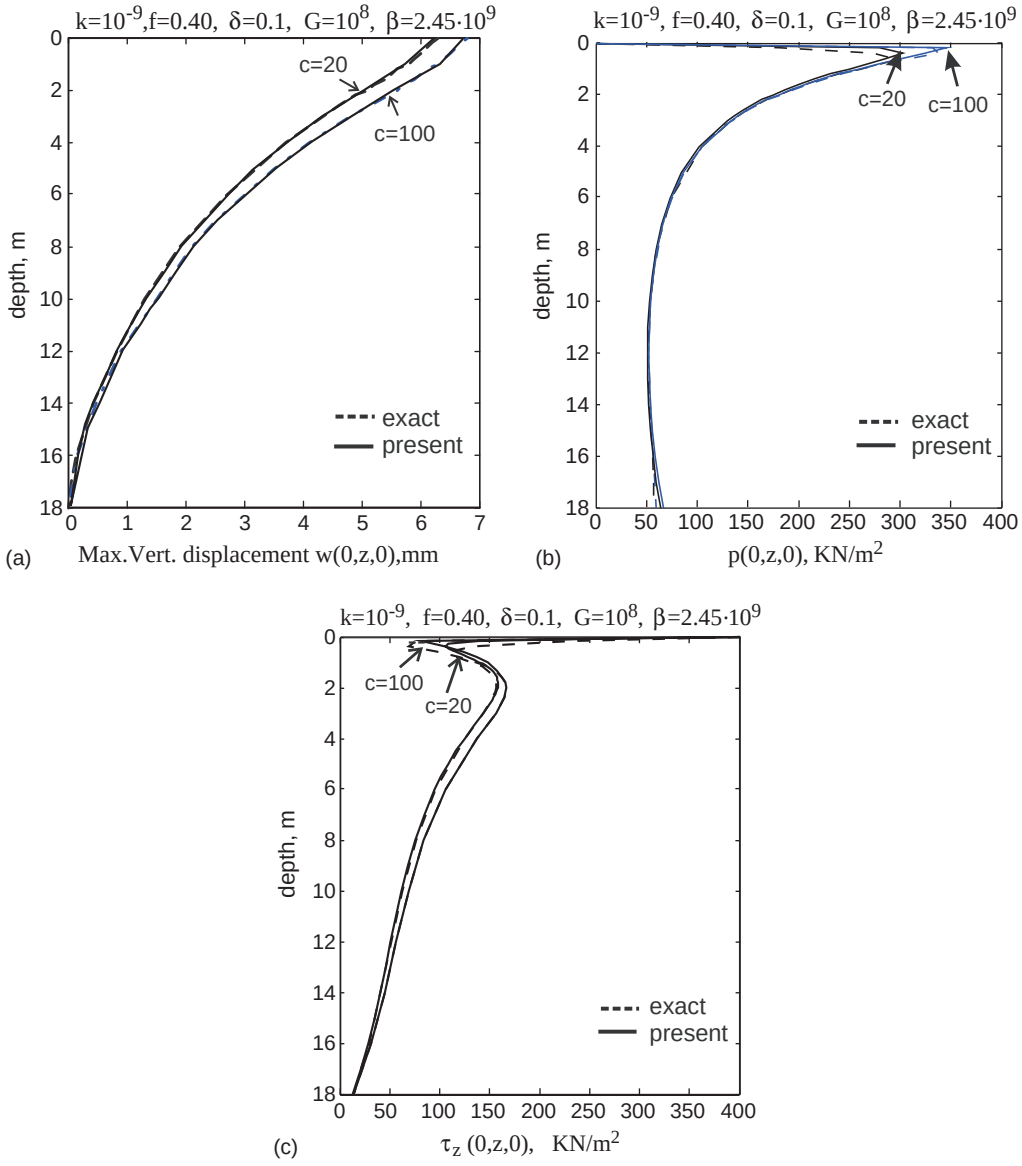

Fig. 5. Comparison of the maximum vertical displacement (a), porewater pressure (b) and vertical effective stress (c) between the present approximate method and exact solution ($k = 10^{-9}$ m^3 s/kg $= 10^{-5}$ m/s, $G = 10^8$ N/m^2).

solution of Theodorakopoulos (2003), for $G = 10^8$ N/m^2, $k = 10^{-9}$ m^3 s/kg $= 10^{-5}$ m/s and for two values of load velocity c (20, 100 m/s) in each figure. It can be seen that the agreement between the two solutions is very satisfactory for all three response functions. These conclusions are the consequence of the fact that in the case of a fine material ($k = 10^{-9}$ m^3 s/kg $= 10^{-5}$ m/s) the values of $R_{n=1}$ and $H/d_{n=1}$ are much larger than unity, as required by the theory of Mei and Foda (1981). Furthermore, it is observed from Fig. 5(a)–(c), that for $c = 100$ m/s, the agreement between the two solutions has been even more satisfactory due to even more larger values of the quantities $R_{n=1}$ and $H/d_{n=1}$ computed in such a case.

The comparison of the response of the soil medium under moving loads between the present approximate method and the exact solution for the case of a coarse material ($k = 10^{-7}$ m^3 s/kg $= 10^{-3}$ m/s), is shown in Fig. 6(a)–(c), again for two values of load velocity c (20, 100 m/s) in each figure. One can see that the agreement between the two solutions, as far as the vertical displacement is concerned, Fig. 6(a), is yet excellent, although for the coarse material the depth of the boundary layer $d_{n=1}$ is not small compared to the layer depth H (Table 2). Moreover, the same conclusion can be drawn for the case of a softer material, as

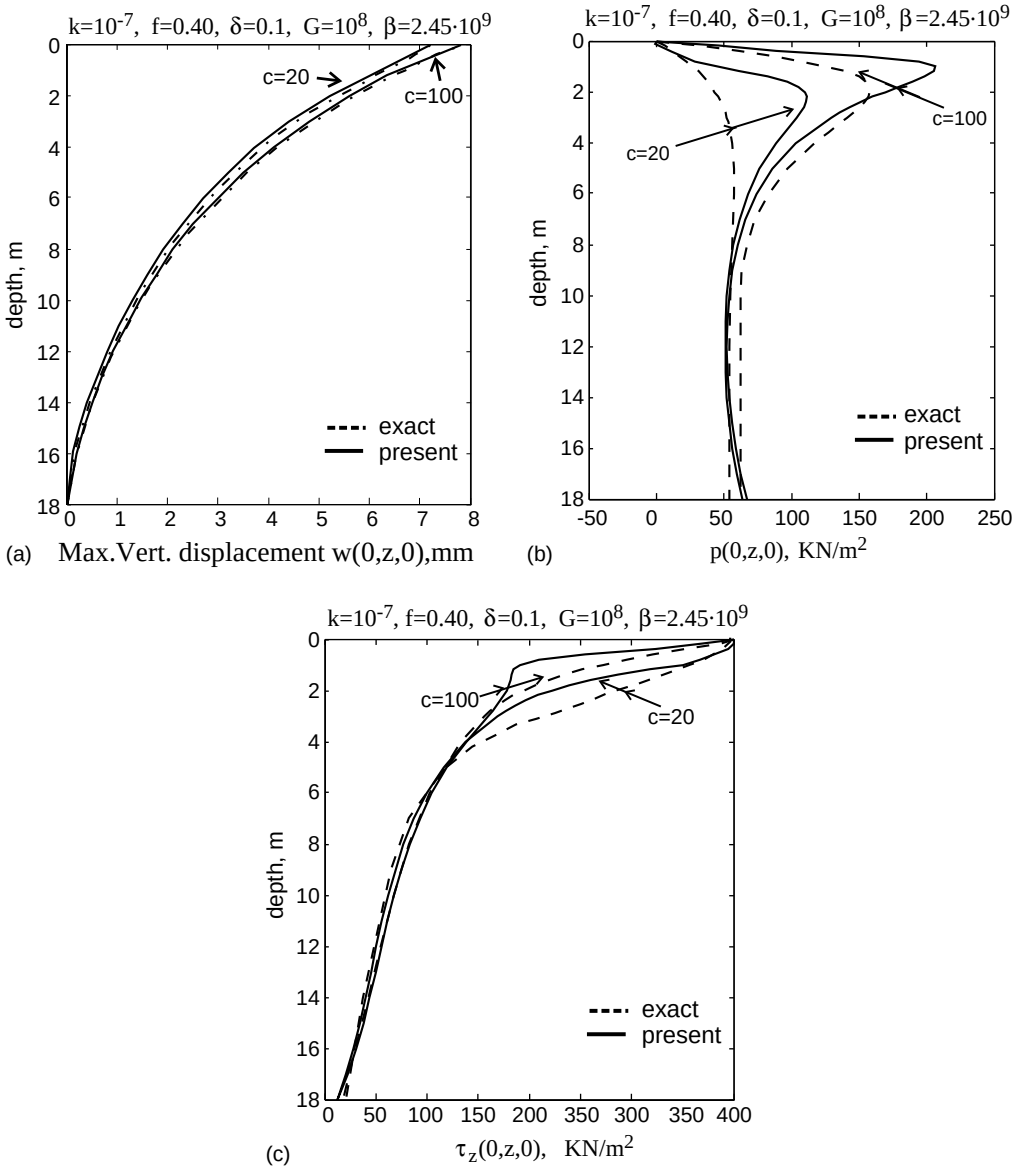

Fig. 6. Comparison of the maximum vertical displacement (a), porewater pressure (b) and vertical effective stress (c) between the present approximate method and exact solution ($k = 10^{-7}$ m^3 s/kg $= 10^{-3}$ m/s, $G = 10^8$ N/m^2).

shown in Fig. 7, where the vertical displacement is plotted versus depth for two values of permeability, $c = 20$ m/s and $G = 0.2 \times 10^8$ N/m^2.

However, referring back to Fig. 6(b) and (c), it can be observed that, for a coarse material, there is a discrepancy in both the porewater pressure and the vertical solid effective stress between the two solutions. More specifically, the use of the present approximate method overestimates the porewater pressure and, as an expectation, underestimates the vertical solid effective stress. These discrepancies for the case of $k = 10^{-7}$ m^3 s/kg $= 10^{-3}$ m/s can be attributed to the large depth of the boundary layer, which seems to affect the distribution of the applied load between solid and fluid more than it affects the overall response of the vertical displacement when the present method is used. It should be reminded that the value of the ratio $H/d_{n=1}$ increases proportionally to the square root of c, and this explains the smaller discrepancies in p and τ_z between the two solutions when the load velocity increases from $c = 20$ to 100 m/s, respectively, as shown in Fig. 6(b) and (c).

Bearing in mind the above results and having a closer inspection of Figs. 3(a)–(b) and 4(a)–(b), one can conclude that a satisfactory agreement between the two solutions, is expected, as far as the porewater pressure and the vertical solid effective stress are concerned, if and only if the total response of the medium is governed by the outer approximation solution of the present method, and this occurs in the case of a fine material.

As mentioned before, there exists an excellent agreement of the displacement response between the present approximate method and the exact solution of Theodorakopoulos (2003) for both fine and coarse materials and for any range of load speed within the limits used in practice, ($c = 100$ m/s $= 360$ km/h). This is also demonstrated in Table 3, where the maximum surface displacement values are calculated for various values of the poroelastic material properties and velocity c. It can be seen that for a hard solid material, $G = 10^8$ N/m^2, the agreement between the two solutions is yet excellent even for more permeable material, $k = 10^{-6}$ m^3 s/kg $= 10^{-2}$ m/s, for which $d_{n=1} > H$. It is of interest to note that the largest value of load speed considered in these calculations, $c = 100$ m/s, has been a rather small percentage of the shear wave velocity $v_s = \sqrt{G/\rho_s} = 234.66$ m/s. Also, in the case of $G = 10^8$ N/m^2, the effect of porosity is negligible when the

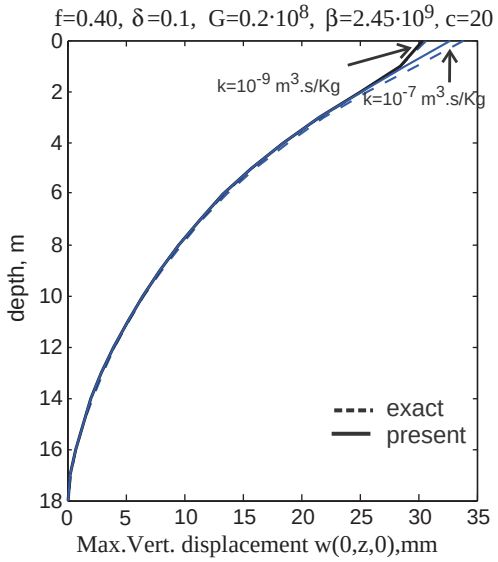

Fig. 7. Comparison of the maximum vertical displacement between the present approximate method and the exact solution ($c = 20$ m/s, $G = 0.2 \times 10^8$ N/m^2).

Table 3
Comparison of the maximum vertical surface displacement between the present approximate method and the exact solution for various values of permeability, porosity, shear modulus and load velocity

	c	c/U_s, %	Exact solution		Present solution			
			$f = 0.20$	$f = 0.40$	$f = 0.20$		$f = 0.40$	
			w	w	w^o	w	w^o	w
$G = 10^8$ $v_s = 234.66$ m/s (845 km/h)								
$k = 10^{-9}$ m^3 s/kg $= 10^{-5}$ m/s	20	9	6.1	6.2	5.7	6.1	5.7	6.2
	65	28	6.2	6.3	5.9	6.3	5.9	6.3
	80	34	6.4	6.5	6.0	6.4	6.1	6.4
	100	43	6.7	6.6	6.3	6.6	6.3	6.6
$k = 10^{-7}$ m^3 s/kg $= 10^{-3}$ m/s	20	9	7.5	7.5	5.7	7.1	5.7	7.2
	65	28	7.1	7.1	5.9	6.9	5.9	6.9
	80	34	7.2	7.2	6.0	6.9	6.1	6.9
	100	43	7.4	7.2	6.3	7.1	6.3	7.1
$k = 10^{-6}$ m^3 s/kg $= 10^{-2}$ m/s	20	9	8.7	8.7	5.7	8.7	5.7	8.6
	65	28	8.6	8.5	5.9	8.3	5.9	8.2
	80	34	8.6	8.6	6.0	8.2	6.1	8.2
	100	43	8.7	8.4	6.3	8.3	6.3	8.2
$G = 0.35 \times 10^8$ $v_s = 138.83$ m/s (500 km/h)								
$k = 10^{-9}$ m^3 s/kg $= 10^{-5}$ m/s	20	14	17.3	17.4	16.1	17.2	16.2	17.3
	65	47	19.0	19.1	18.2	19.2	18.0	19.0
	80	58	20.0	18.9	19.7	20.7	19.3	20.3
	100	72	22.7	22.2	23.2	24.2	22.2	23.2
$k = 10^{-7}$ m^3 s/kg $= 10^{-3}$ m/s	20	14	19.9	19.9	16.1	19.1	16.2	19.1
	65	47	20.8	20.6	18.2	20.2	18.0	20.1
	80	58	21.9	21.8	19.7	21.7	19.3	21.3
	100	72	23.2	21.6	23.2	25.1	22.2	24.1
$k = 10^{-6}$ m^3 s/kg $= 10^{-2}$ m/s	20	14	24.1	24.1	16.1	23.5	16.2	23.4
	65	47	23.5	23.0	18.2	22.8	18.0	22.5
	80	58	24.3	24.3	19.7	24.0	19.3	23.5
	100	72	26.3	24.0	23.2	27.4	22.2	26.2
$G = 0.20 \times 10^8$ $v_s = 104.94$ m/s (378 km/h)								
$k = 10^{-9}$ m^3 s/kg $= 10^{-5}$ m/s	20	19	30.4	30.4	28.4	30.3	28.5	30.3
	65	62	36.5	36.4	35.8	37.6	34.8	34.8
	80	76	41.6	41.3	43.3	45.0	40.8	42.5
	100	95	53.9	46.3	70.6	72.4	61.3	63.1
$k = 10^{-7}$ m^3 s/kg $= 10^{-3}$ m/s	20	19	33.8	33.8	28.4	32.7	28.5	32.7
	65	62	37.5	35.9	35.8	39.0	34.8	38.0
	80	76	41.6	40.3	43.3	46.4	40.8	43.9
	100	95	71.1	59.5	70.6	74.2	61.3	64.7
$k = 10^{-6}$ m^3 s/kg $= 10^{-2}$ m/s	20	19	40.6	40.5	28.4	38.6	28.5	38.5
	65	62	44.2	44.0	35.8	42.5	34.8	41.5
	80	76	53.0	48.8	43.3	49.9	40.8	47.2
	100	95	96.4	71.7	70.6	78.6	61.3	68.6

present method is used, in agreement with the case of the exact solution (Theodorakopoulos, 2003). Similar conclusions can be drawn for the case of $G = 0.35 \times 10^8$ N/m^2 as far as the agreement of the values of the

maximum surface displacement obtained by the two solutions is concerned. However, in an even softer medium with $G = 0.2 \times 10^8$ N/m^2, the effect of increasing values of permeability and porosity on the above mentioned agreement is apparent, especially in the range of high speeds, for reasons explained in Theodorakopoulos (2003).

The relationship of the surface vertical displacement responses for the outer approximation and the total field solutions of the present method is also of practical value. From the computed values of w^o and w in Table 2 the following are noted:

- For any soil medium, increasing w^o/w ratios are found with increasing values of load velocity.
- For a soil medium with a given value of G, the w^o/w ratio decreases with increasing permeability, since the value w^o is constant, i.e., independent of the value of k. Similarly, for a given permeability, the w^o/w ratio increases with decreasing value of G.
- The effect of porosity on the value of w^o is only apparent in the case of soft materials with high permeability, especially in the range of high load speeds.
- For a fine soil medium ($k = 10^{-9}$ m^3 s/kg $= 10^{-5}$ m/s) and low values of c, the ratio w^o/w is of about 94%, whereas for a coarse material ($k = 10^{-7}$ m^3 s/kg $= 10^{-3}$ m/s) the corresponding w^o/w ratio decreases to about 80%.

Thus, as mentioned before, it can be concluded, that for a fine material and for the whole range of the load speeds, the displacement response of the soil layer can be found by only using the outer approximation solution.

The comparison between the two solution procedures for the porewater pressure at 2.0 m depth and at a horizontal distance $x = 160$ m from the origin is shown in Fig. 8(a) and (b) for two values of permeability and a specific value of load velocity in each figure. One can see that, for a high value of permeability and for both values of load velocity, the agreement between the two solutions is very satisfactory, as expected. In

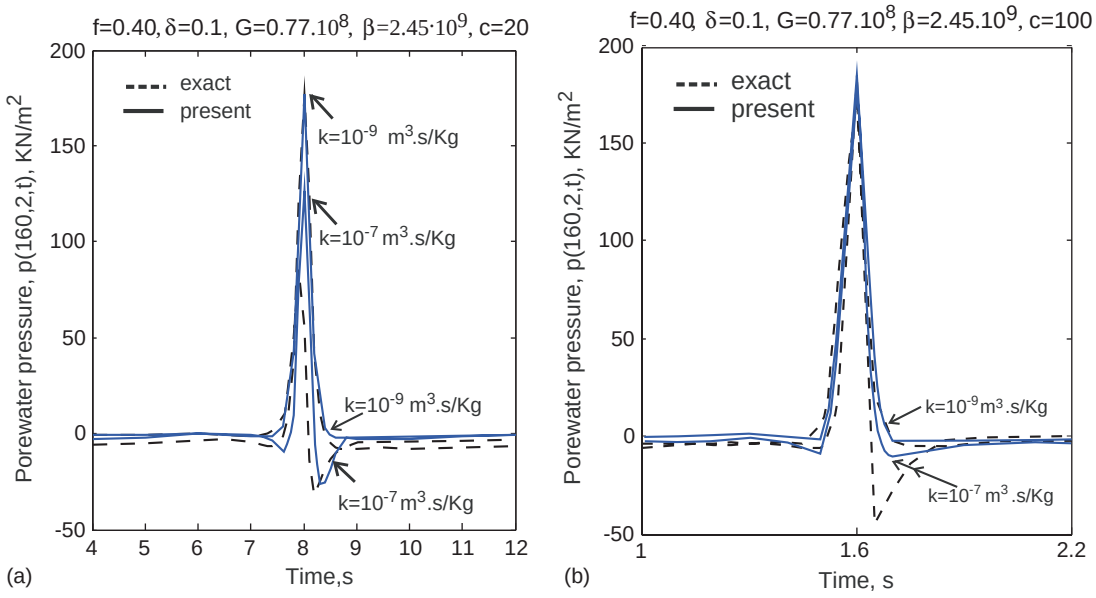

Fig. 8. Comparison of the porewater pressure at 2.0 m depth between the present approximate method and exact solution for various values of k and $c = 20$ m/s (a) and $c = 100$ m/s (b).

addition, the maximum fluid pressure for both solutions occurs at $t = 8$ and 1.6 s, which are the traveling times of the moving load up to the plane of observation, AA (Fig. 1), for $c = 20$ and 100 m/s, respectively. However, for a more permeable material ($k = 10^{-7}$ m^3 s/kg $= 10^{-3}$ m/s) and at low speeds, Fig. 8(a), two differences in porewater pressure response can be observed. The first one has to do with the magnitude of peak response, being larger when the present approximate method is used, and the second one pertains to the time at which these peaks occur. One can see that, in the exact solution, the maximum fluid pressure occurs at a little bit earlier time than that of $t = 8$ s ($t = 160$ m/20 m/s) for reasons explained in Theodorakopoulos (2003). As far as the negative profile of the porewater pressure as the load moves away from the point of interest is concerned, the two solutions exhibit similar response for $k = 10^{-7}$ m^3 s/kg $= 10^{-3}$ m/s. This porewater pressure behavior is consistent with earlier theoretical analysis (Siddharthan et al., 1993; Burke and Kingsbury, 1984). However, this consistency between the two solutions in the negative values of pressure is not longer true for $c = 100$ m/s, as shown in Fig. 8(b).

Based on the above stated differences in the porewater pressure responses as computed by both the present approximate method and the exact solution, and bearing in mind the corresponding comparisons in Theodorakopoulos (2003) between the exact solution and the method proposed by Siddharthan et al. (1993), it can be said that for a fine material the response behavior between the pressure of approximate solution and that of Siddharthan et al. (1993) is similar. This is due to the fact that, in such a case, the response of the present approximate method is governed by the outer approximation solution and, hence, both solution procedures are based on the same assumption, that is, of no relative motion between solid and fluid constituents.

Fig. 9 shows the solid vertical effective stress at 2.0 m depth below the point of interest at $x = 160$ m for $k = 10^{-9}$ m^3 s/kg $= 10^{-5}$ m/s and $c = 20$ m/s. It can be seen that the agreement in the responses between the present method and the exact solution is excellent as the load approaches and moves away from the plane of observation (Fig. 1).

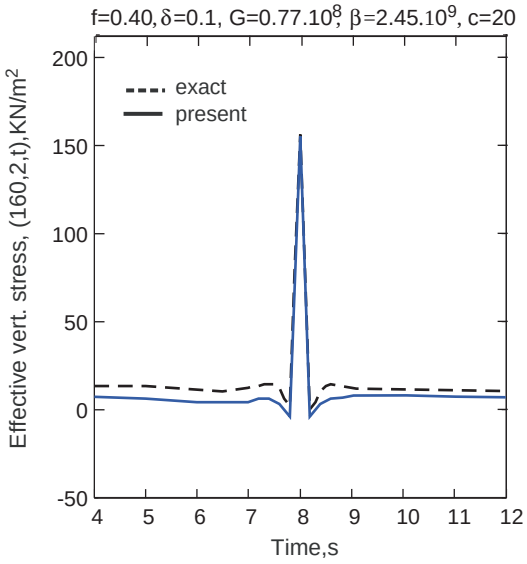

Fig. 9. Comparison of the vertical effective stress at 2.0 m depth between the present approximate method and exact solution ($k = 10^{-9}$ m^3 s/kg $= 10^{-5}$ m/s, $c = 20$ m/s).

6. Conclusions

On the basis of the preceding developments, the following conclusions can be drawn:

1. The problem of the dynamic response of a fully saturated poroelastic soil layer on bedrock subjected to a moving strip load on its surface was solved analytically in an approximate way under conditions of plane strain.
2. The method of solution was based on the theory of Mei and Foda. The solid vertical displacement, porewater pressure and solid vertical effective stress were explicitly expressed as the sum of the outer approximation problem and the boundary layer correction. Their variation with the various parameters of the problem such as shear modulus, permeability, porosity and load velocity was numerically computed.
3. In the case of a soil medium with low permeability ($k = 10^{-5}$ m/s), the vertical displacement response found by the outer approximation solution is of about 95% of the total response and, hence, the boundary layer correction can be neglected for engineering purposes.
4. Similarly, for a soil material with low permeability, the effect of the boundary layer correction on the porewater and solid vertical effective stress responses is negligible, except near the free surface where the boundary layer correction gives the expected distributions due to the boundary conditions.
5. However, for a more permeable material ($k = 10^{-3}$ m/s), the effect of the boundary layer correction on the response was found to be significant, especially in the cases of porewater pressure and vertical effective stress.
6. The accuracy of the present approximate method has been demonstrated by comparing its predictions with those obtained by the exact solution. The numerical data that have been presented provide a framework for the range of the material properties for which the present method can be used. Thus,
   (i) For a fine material and almost independently of the value of the shear modulus of the soil medium, the agreement between the present method and the exact solution for any response function is very satisfactory.
   (ii) For a coarse material, the accuracy of the present method in relation to the vertical displacement is very satisfactory but there exist discrepancies in relation to porewater pressure and solid vertical effective stress responses between the present and exact solutions.
   (iii) The accuracy of the present method compared with the exact solution becomes more pronounced with increasing load velocity for any range of the values of material properties, except in the case of a soft material at high speeds.
7. The approximate method presented herein provides an alternative method of analysis of a poroelastic soil medium under moving loads characterized by simplicity, less computational effort and high accuracy, especially in the case of fine materials.

References

Biot, M.A., 1956. Theory of propagation of elastic waves in a fluid-saturated porous solid. Part I: Low-frequency range; Part II: High-frequency range. Journal of the Acoustical Society of America 28, 168–191.

Burke, M., Kingsbury, H.B., 1984. Response of poroelastic layers to moving loads. International Journal of Solid and Structures 20 (5), 499–511.

Foda, M.A., Mei, C.C., 1983. A boundary layer theory for Rayleigh waves in a porous fluid-filled half-space. Soil Dynamics and Earthquake Engineering 2, 62–65.

Kattis, S.E., Karabalis, D.L., Beskos, D.E., 1998. Effects of poroelastic saturated soil on the seismic response of tunnels. In: Bisch, P., Labb, P., Pecker, A. (Eds.), Proceedings of 11th European Conference on Earthquake Engineering Paris. A.A. Balkema, Rotterdam, p. 998 (abstract), CD Rom (full text).

Kattis, S.E., Karveli, K., Karabalis, D.L., Beskos, D.E., 1999. Seismic response analysis of lined tunnels in poroelastic soil medium. In: Oliveto, G., Brebbia, C.A. (Eds.), Earthquake Resistant Engineering Structures II. WIT Press, Southampton, pp. 615–624.

Kattis, S.E., Beskos, D.E., Cheng, A.H.D., 2003. 2-D dynamic response of unlined and lined tunnels in poroelastic soil to harmonic body waves. Earthquake Engineering and Structural Dynamics 32, 97–110.

Mei, C.C., Foda, M.A., 1981. Wave-induced responses in a fluid-filled poroelastic solid with a free surface—a boundary layer theory. Geophysical Journal of the Royal Astronomical Society 66, 597–631.

Mei, C.C., Si, B.I., Cai, D., 1984. Scattering of simple harmonic waves by a circular cavity in a fluid-infiltrated poroelastic medium. Wave Motion 6, 265–278.

Siddharthan, R., Zafir, Z., Norris, G.M., 1993. Moving load response of layered soil. Part I: Formulation; Part II: Verification and application. Journal of Engineering Mechanics, ASCE 119 (10), 2052–2089.

Theodorakopoulos, D.D., 2003. Dynamic analysis of a poroelastic half-plane soil medium under moving loads. Soil Dynamics and Earthquake Engineering 23, 521–533.

Theodorakopoulos, D.D., Chassiakos, A.P., Beskos, D.E., 2001. Dynamic pressures on rigid cantilever walls retaining poroelastic soil media. Part I: First method of solution, Part II: Second method of solution. Soil Dynamics and Earthquake Engineering 21, 315–364.